



LAWRENCE
LIVERMORE
NATIONAL
LABORATORY

UCRL-CONF-155818

NIF Commissioning and Initial Performance Results

*B. M. Van Wonterghem, S. C. Burkhart, C. A.
Haynam, K. R. Manes, C. D. Marshall, J. E.
Murray, M. L. Spaeth, D. R. Speck, S. B.
Sutton, and P. J. Wegner*

December 19, 2003

Society of Photo-Optical Instrumentation Engineers
Photonics West – LASE 2004 Conference, San Jose,
California, January 24-29, 2004

This document was prepared as an account of work sponsored by an agency of the United States Government. Neither the United States Government nor the University of California nor any of their employees, makes any warranty, express or implied, or assumes any legal liability or responsibility for the accuracy, completeness, or usefulness of any information, apparatus, product, or process disclosed, or represents that its use would not infringe privately owned rights. Reference herein to any specific commercial product, process, or service by trade name, trademark, manufacturer, or otherwise, does not necessarily constitute or imply its endorsement, recommendation, or favoring by the United States Government or the University of California. The views and opinions of authors expressed herein do not necessarily state or reflect those of the United States Government or the University of California, and shall not be used for advertising or product endorsement purposes.

NIF commissioning and initial performance results*

B. M. Van Wonterghem, S.C. Burkhart, C.A Haynam, K.R. Manes, C.D. Marshall,
J.E. Murray, M.L. Spaeth, D.R. Speck, S.B. Sutton and P. J. Wegner,
NIF Project, Lawrence Livermore National Laboratory, Livermore, CA, USA, 94550

ABSTRACT

The National Ignition Facility at LLNL recently commissioned the first set of four beam lines into the target chamber. This effort, also called NIF Early Light, demonstrated the entire laser system architecture from master oscillator through target and initial X-ray diagnostics. This paper describes the detailed commissioning and installation steps for one of NIF's 48 beam quads. Using a dedicated single beam line Precision Diagnostic System, performance was explored over the entire power versus energy space from 6.4 TW/beam for sub-nanosecond pulses to 25 kJ/beam for 23 ns pulses at 1ω . NEL also demonstrated record single beam line frequency converted Nd:Glass laser energies of 11.3 kJ at 2ω and 10.4 kJ at 3ω .

Keywords: Solid state lasers, Neodymium, Fusion lasers

1. INTRODUCTION

The NIF Facility is designed as a 192 laser beam target irradiation facility to perform inertial confinement fusion and weapons physics experiments in support of the U.S. Stockpile Stewardship Program. When completed it will provide the capability to irradiate targets with several megajoules of laser energy in precisely controlled spatial and temporal profile ranging from 0.2 to 25 ns. NIF's performance will exceed the capabilities of current large Nd:Glass facilities by a factor of fifty. The design of NIF is the culmination of over 25 years of laser development and operation at the

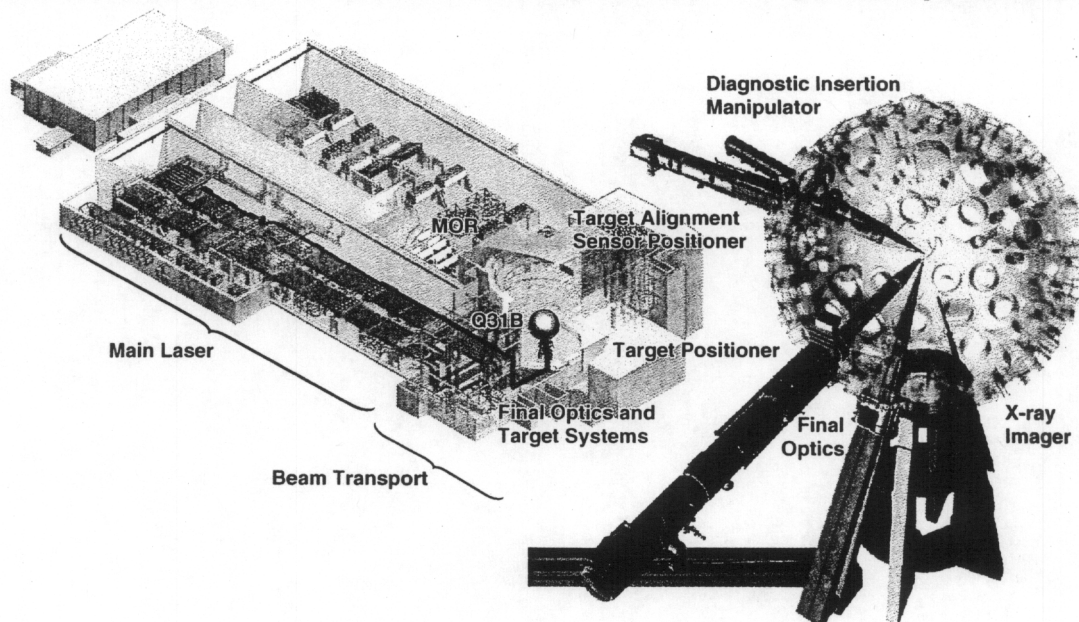


Fig. 1. The NIF Early Light Project commissioned the first beam quad (Quad 31B) all the way from the master oscillator to the target chamber. The inset on the right shows the location of the final optics for the first quad, along with target alignment, positioning and initial diagnostic systems used as part of commissioning.

*Work performed under the auspices of the U.S. Department of Energy by Lawrence Livermore National Laboratory under Contract No W-7405-Eng-48

Lawrence Livermore National Laboratory. In April 2001, the NIF project started an effort to install and commission the first set of 4 beam lines to test and validate the entire system design from the Master Oscillator (MOR) generating the initial temporal pulse shape, through the main laser and into a target located at the center of a massive 10 meter diameter target chamber. This project was called NIF Early Light (NEL). The remainder of this paper describes the details of the laser commissioning sequence for this quad of beam lines and some initial performance results.

NIF's 192 beamlines are arranged into four clusters of 48 beam lines. Each cluster consists of 6 bundles. Each bundle contains eight beams which share a common 4x2 aperture laser amplifier system. Each bundle is made up of two quads, having an independent pulse shaping and preamplifier system. After propagating through a common main laser amplifier in the laser bays, the bundles are physically split into two quads of 2x2 beam lines which are subsequently redirected to individual final optics unit located on the target chamber.

The NEL demonstration took place on the bottom quad of bundle 31, which is the first bundle of the third cluster in the 2nd laser bay. Fig. 1 shows the location of this quad of beam lines within the facility. NEL tested the unit cells of every laser subsystem: one quad of laser beam lines within a complete bundle based laser amplifier (4 beam apertures high by 2 wide), and a full cluster of beampath infrastructure, support systems and utilities in the laser bay and switchyard.

1. LRU INSTALLATION AND ALIGNMENT COMMISSIONING

The commissioning of the NIF laser is quite unique as a consequence of the laser multi-pass architecture and the Line Replaceable Unit (LRU) based mounting of optical components. Previous fusion lasers were based on discrete beam lines and individual opto-mechanical components mounted on large space frames with easy access and individual adjustments. The NIF laser required the use of LRU's that to achieve the required high packing density. This precludes easy access to optical units after installation. LRU's are inserted by robotic transporters into kinematic mounts located on the supporting infrastructure. Tight component centering ($\sim 1\text{mm}$) and pointing tolerances are achieved by precise laser based surveying of kinematic mounts, and off-line pre-alignment of optical components within the LRU structure. Individual kinematic mounts and large support structures (up to 40 ton vessels) were positioned to better than $200\text{ }\mu\text{m}$ with state-of-the-art laser surveying. A robotic alignment verification system located in the LRU assembly facility demonstrated optical surface pre-alignment to better than $50\text{ }\mu\text{r}$. Reference LRUs are used in the transport spatial filter to align centering light sources and diagnostics and alignment beam paths to the output sensor.

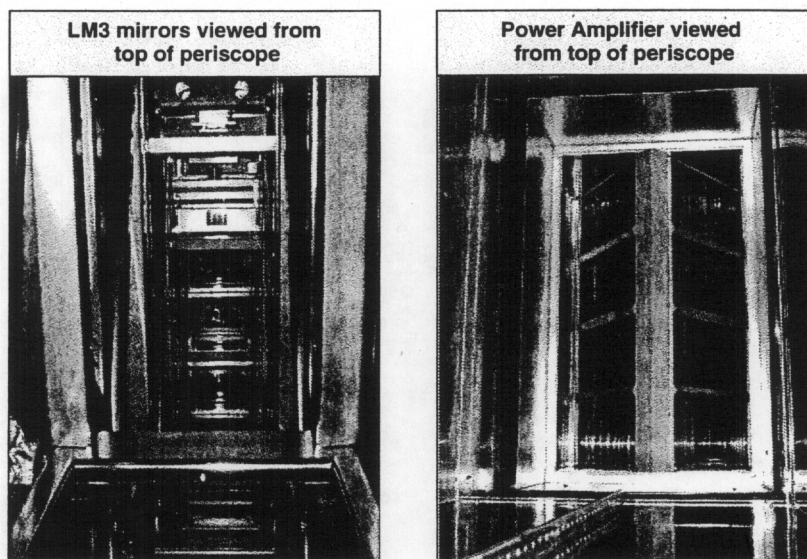


Fig. 2: Internal views of the optical components and LRU structures inside the main laser beampath

In addition, the high laser fluences generated in NIF impose strict cleanliness requirements on the beampath infrastructure components and optical surfaces. NEL demonstrated that we could achieve these cleanliness requirements of the integrated system using a combination of high throughput state-of-the-art cleaning facilities for beampath and optical components along with clean-room construction protocols and transport of LRU's in clean room type canisters. To further enhance the cleanliness, the flashlamps of the cavity and power amplifiers are fired for 10-50 shots in the empty beampath to burn off any remaining organic films on the beampath surface areas. Volatilized material is purged by a high flow of clean dry air through these beampath sections. The clean installation and subsequent flashlamp cleaning resulted in amplifier slab conditions that were one order of magnitude better than the Beamlet prototype¹, with surface densities below $10/\text{ft}^2$ for obscurations larger than $100\text{ }\mu\text{m}$.

Fig. 2 shows a beampath view of the periscope (a section of the main laser cavity containing the beam injection polarizers and turning mirrors) and the main laser amplifier, showing the 4x2 laser slab configuration, pumped by 3 sets of flashlamp, located on each side of the slabs. These sections were completely built out for the NEL system.

2. MAIN LASER COMMISSIONING

This section highlights the major main laser commissioning steps following LRU installation. Fig. 3 shows these steps using schematic diagrams of the optical beam line as it propagates from MOR to the Injection Laser System (ILS), through the main laser into the switchyard transport mirrors and the target chamber.

Once most of the main laser optical component LRUs were installed, alignment of the Input Sensor (ISP) alignment beam was completed through the Preamplifier Beam Transport Optics (PABTS) into the Transport Spatial Filter (TSF,

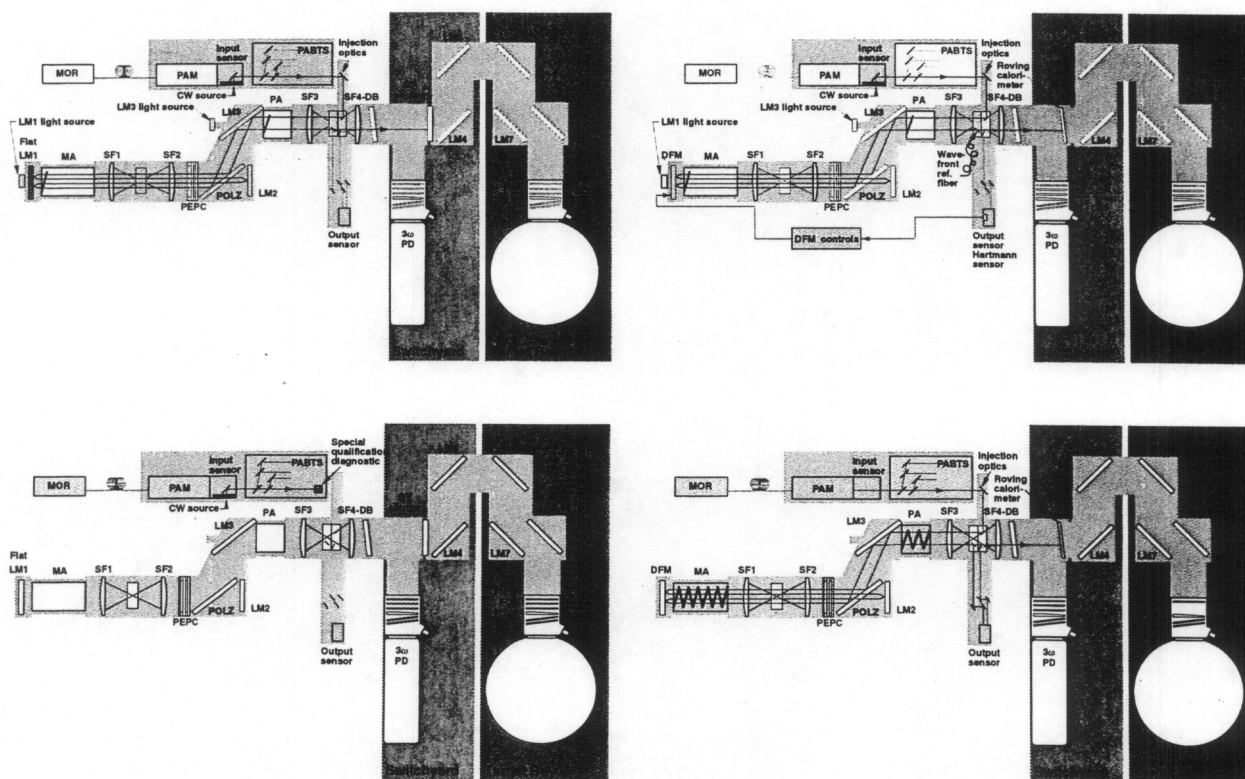


Fig. 3. Major steps in the main laser commissioning: beam alignment (top left), wavefront control activation (top right), Injection laser commissioning (lower left), and pulsed operation commissioning (lower right)

consisting of SF3 and 4), and the main laser cavity. The 4-pass cavity consists of the main amplifier (MA), a relaying cavity spatial filter (CSF) and two cavity mirrors, LM1 and LM2. After 4 passes the beam is sent back through the power amplifier (PA) towards the transport mirrors in the switchyard through the TSF. The output sensor (OSP) is used as both alignment sensor and output diagnostic system for the main laser. Alignment commissioning requires calibration and test of 11 individual alignment loops using software maintenance panels and the auto-alignment controls. As opposed to previous laser systems, this activity does not require component location adjustments, and we demonstrated the design clear aperture of the system (400 x 400 mm²), while propagating pulsed beam sizes between 360 and 373 mm (1% intensity edge) with an equivalent area of >1150 cm². The pointing stability of the beams at the output of the TSF were better than 0.5 μ R RMS. Details of the alignment system are described elsewhere in these proceedings².

Once main the main laser was optically aligned, the wavefront control loop activation and test proceeded. The wavefront control system consists of a full aperture 39 element deformable mirror located in the multi-pass cavity, a Shack-Hartmann wavefront sensor located in the OSP and a real time control system². Corrected output wavefronts of the NEL chains running in closed loop show an RMS error typically smaller than 0.25 waves, as shown in Fig. 4

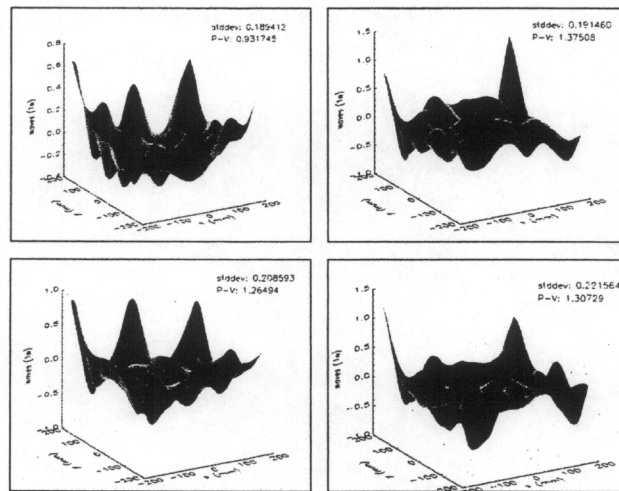


Fig. 4. Residual wavefront error of the main laser beamlines after correction for static aberrations.

While main laser alignment proceeded, the Injection Laser System was prepared for operation. The Preamplifier Module (PAM) was assembled and tested off-line in a dedicated test and maintenance facility, before being installed in its support structure in the laser bay. The PAM was then connected to the master oscillator fiber delivery system, and the ISP diagnostic system and beam transport. A dedicated set of diagnostics is used for operational qualification of the four PABTS beam lines prior to injection in the main amplifier cavity. The test includes validation of energetics, beam balance, near field, focal spot and wavefront (collimation). More details on the ILS system are described elsewhere in these proceedings³. The ILS typically provides spatially, temporally and spectrally shaped pulses to compensate for downstream gain saturation, gain profile variations and gain dispersion. Typical amplitude modulation of the pulse as a result of the frequency modulation imposed on the beam to protect against SBS and for spectral beam smoothing (4), were below 10% pk-pk using a novel AM-FM compensator device.

Once main laser alignment and the injection laser system were operational, commissioning of the pulsed operations commenced. First, low energy PAM shots were fired through the main laser into the output sensor to set system timing and validate performance of the Plasma Electrode Pockels Cell in the multi-pass cavity^{5,6}. Subsequently the main laser was fired into a set of full aperture calibration calorimeters in the roving calorimeter enclosure located at the entrance of the switchyard. The main laser operational qualification was completed by firing the four NEL beams at a total of 43 kJ (3.5 ns), with a beam energy balance of $\pm 1\%$. Fig. 5 shows the resulting main laser fluence distributions at the output of the transport spatial filter as captured by the output sensor.

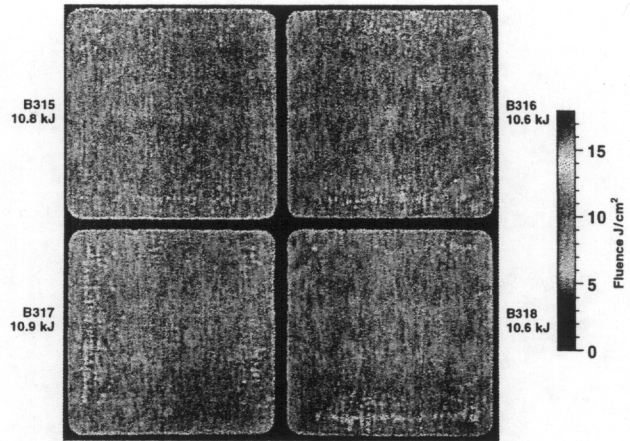


Fig. 5. Four beam near field profile of the 43 kJ main laser commissioning milestone shot

3. BEAM TRANSPORT AND TARGET AREA COMMISSIONING

The beam transport commissioning includes installation and alignment of the transport mirrors located in switchyard and target bay. The target area commissioning includes installation and alignment of the final optics, drive diagnostics and the target chamber systems required to support initial shots: vacuum systems, target chamber service system,

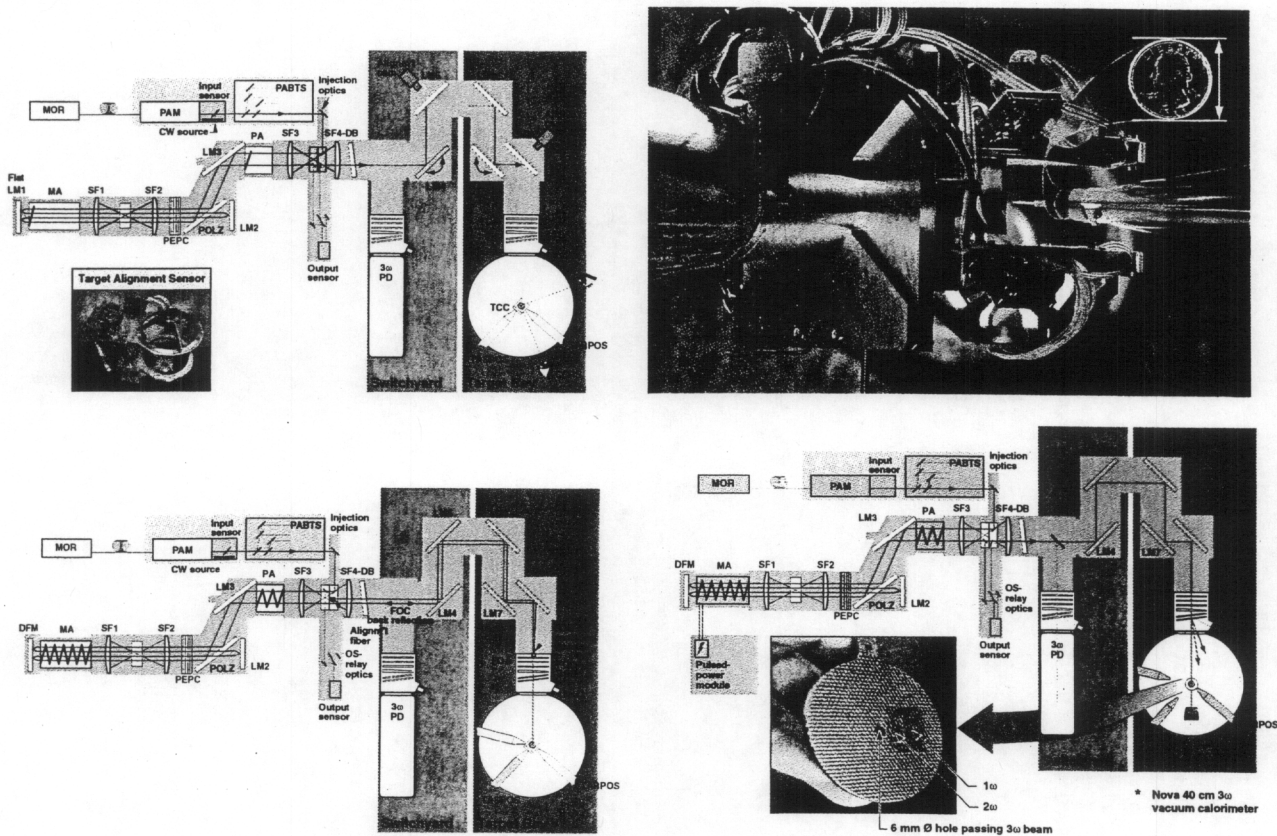


Fig. 6. Major beam transport and target area commissioning steps: transport mirror alignment (UL), target alignment using TAS (UR), beam and final optics alignment (LL), and energy calibration shots to opposed calorimeter through a "puck" target at TCC.

relevant sections of the chamber first wall, and the target alignment and target positioning systems (see Fig.1 insert). A few important steps of the beam transport and target area commissioning are shown in Fig. 6, along with an image of a NIF target held by the target positioner within the jaws of the precision beam and target alignment sensor (TAS).

Beam transport mirror (LM4-8) commissioning involved the use of dedicated alignment LRUs used to precisely set the nominal pointing of the previous mirror in the chain. Once this pointing step is completed, the alignment LRU is replaced by the actual mirror LRU. This LRU is in turn aligned using the next alignment LRU in the chain up to LM8. In the mean time, the final optics enclosures were installed and surveyed. Once the enclosures (also called IOMs) were acceptance tested, the optical elements (vacuum window, frequency converter crystals and final focus lens, beam sampling grating and debris shield) were installed. Next, the 3ω calorimeters and drive diagnostics were aligned.

Once all major systems were installed, beam alignment to target chamber center (TCC) was activated. This involves 2 alignment loops per beam line. The first one points the beams to TCC using a 375 nm alignment source inserted in the transport spatial filter, while centering the incident 1ω beam on the centering fiducials in the final optics cell. The second one aligns the frequency conversion crystal tuning angle by aligning the final focus lens back reflection in the transport filter, functioning as a large scale autocollimator.

After alignment of the beam lines and the final optics, rod shots were fired into the TAS to calibrate the 375 nm alignment light source offsets and the best focus position of the pulsed beam. Once completed, a series of shots was fired into four full aperture calorimeters located on the opposed wall inside the target chamber to validate the beam sampling grating and final optics diagnostic calorimeters. These shots used a large aperture target (puck) located at TCC to block the unconverted 1ω and the 2ω beams. More details on the final optics commissioning and performance are described elsewhere in these proceedings⁷. A subsequent set of campaigns tested beam alignment to target and synchronization of the four beams of the NEL quad using the first NIF X-ray diagnostics: a Static X-Ray Imager (SXI) for alignment, and a Streaked X-Ray Detector (SXD) for beam timing. Initial alignment results of 100 μm RMS met the commissioning goals. Further equipment and procedure improvements will bring this well below 50 μm RMS. Beam timing was set and tested to 6 ps RMS, well within requirements, as shown in Fig. 7.

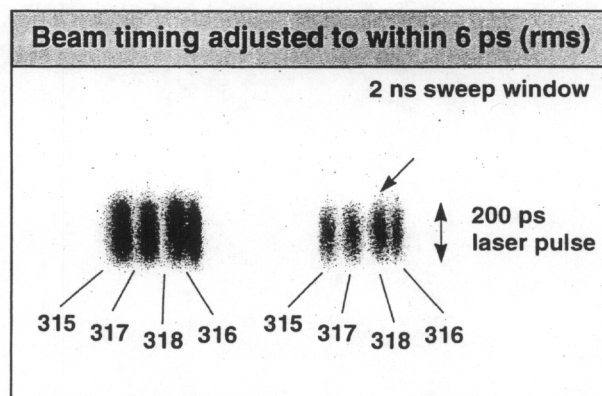


Fig. 7: Beam synchronization of the first four beams using X-ray streak camera images of short pulse shots onto a gold disk target

4. BEAM LINE PERFORMANCE TESTING

Following the operational tests of the NEL laser systems and controls, a set of campaigns was completed to evaluate beam line optical performance. These tests relied heavily on a precision diagnostic system (PDS) located in switchyard 2. Fig. 8 shows a diagram of the PDS, which was designed using the Beamlet prototype 1ω diagnostics and the Focal Plane Diagnostic system⁸. A single beam is selected from the quad using a set of transport mirrors which direct 96% of the light onto a duplicate of the NIF final optics, while the remaining 4% of the light is sent to a set of high resolution

1ω diagnostic systems analyzing near field, far field, wavefront, energy and power. The 3ω diagnostics uses a high resolution vacuum telescope that images the primary focal spot onto a set of five diagnostic tables to diagnose energy, energy balance, power, near field and far field.

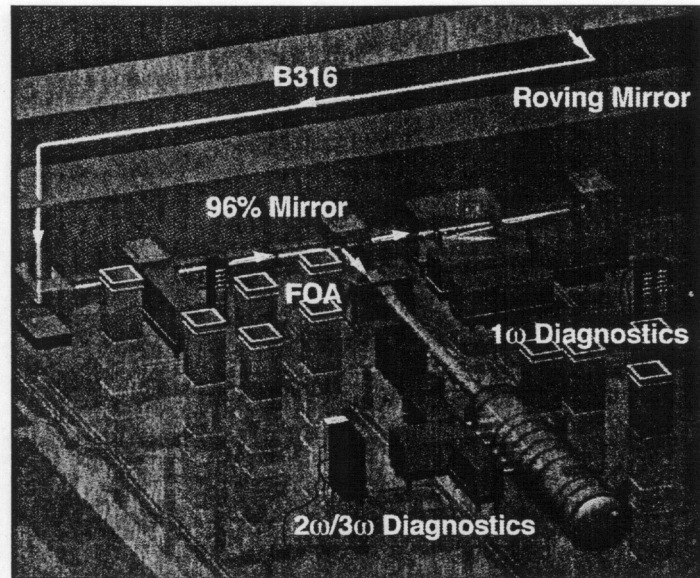


Fig. 8. Layout of the Beamlet Precision Diagnostic system in switchyard 2. Any of the main laser beams can be diverted to PDS by a roving mirror located in the RMDE.

NEL beamline performance was tested over the entire power versus energy design space for flat in time pulses. Fig. 9 shows the calculated limiting performance for the 11 MA slab-7 PA slab configuration pumped at 18% flashlamp explosion fraction, as well as the threshold curve for Stimulated Rotational Raman Scattering (SRRS) in ambient air.

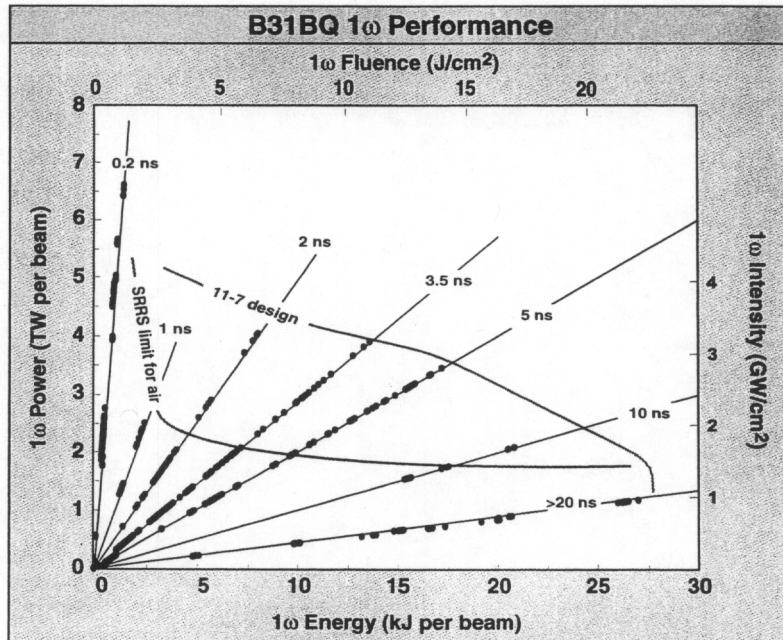


Fig. 9. The main laser testing has explored the entire 1ω flat-in-time pulse performance curve for the 11-7 amplifier configuration from high power operation for short pulses (UL) to high energy operation with 23 ns pulses (LR).

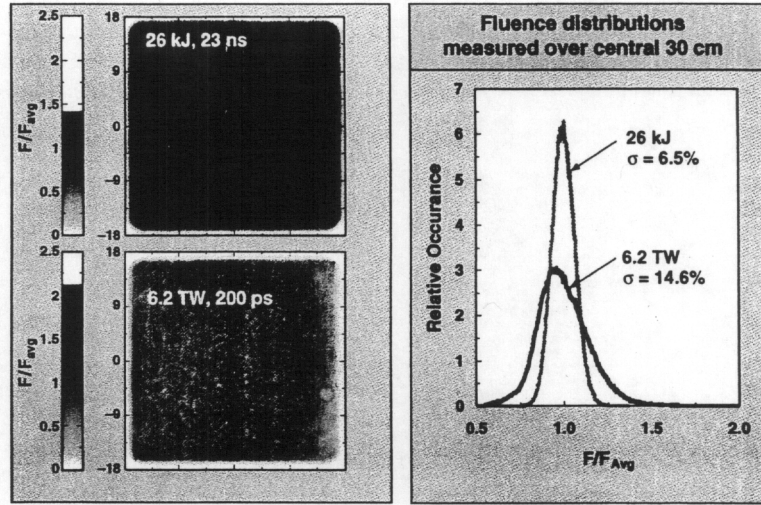


Fig. 10. Near field images and fluence distribution for 1ω beamlines at high power and high energy.

Shots above this line were fired with Argon in the beam transport sections to mitigate SRRS. The points on each straight line represent shot data for different pulse durations, ranging from 220 ps to 23 ns. With 220 psec short pulses, peak powers were generated up to 6.4 TW/beam, while long pulse operation was tested at over 25 kJ/beam using 23 ns pulses. Fig. 10 shows near fields and intensity distributions for typical high power and a high energy shots. The high energy pulse clearly indicates how amplifier saturation flattens the overall spatial fluence distribution and reduces whole beam contrast. Local contrast calculated over a 5 cm central patch was 9.8% for the high intensity pulse, just below the 10% requirement.

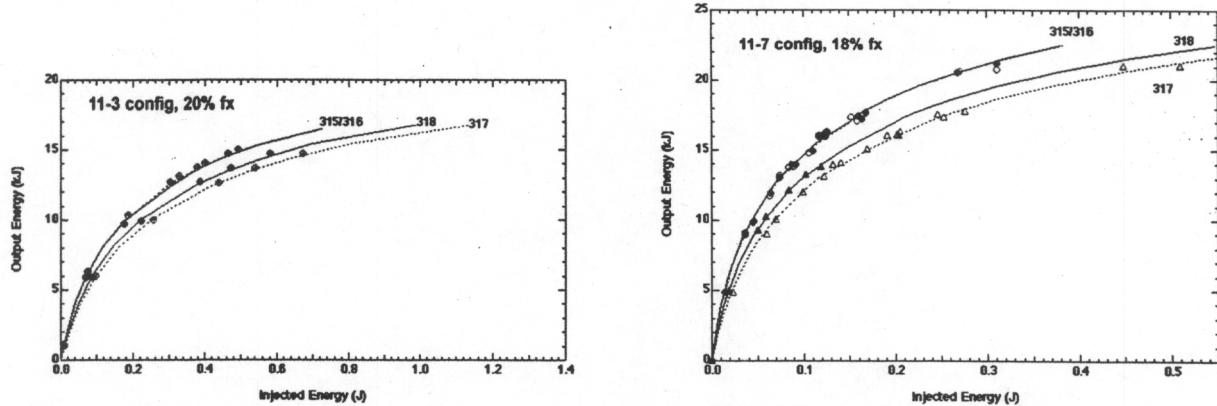


Fig. 11. NEL Quad output energy as a function of injected energy for two different laser amplifier configurations

Amplifier performance was in close agreement with models, as shown in Fig. 11 for two different amplifier configurations, one using 11 main and 3 power amplifier slabs pumped at 20% flashlamp explosion fraction, the second one using 11 cavity and 7 power amplifier slabs pumped at 18% explosion fraction. Details of the NIF laser performance modeling are described in ^{10,11}. The inside apertures of the quad (beams 315 and 316) have a higher gain than the outside apertures (beams 317 and 318) in the amplifiers.

Frequency conversion and performance at high fluences were tested at 2ω and 3ω using the final optics unit in PDS, which is identical to the units mounted on the target chamber. The frequency converter is a conventional Type 1/Type II design with an 11 mm KDP doubler, and a 9 mm deuterated KDP tripler. The design is optimized for best performance at 3 GW/cm^2 drive intensity providing sufficient dynamic range to meet both long, high contrast shaped

ignition pulses as high intensity short pulses. The frequency conversion of the 4 beamlines into the target chamber has been run at 3ω energies over 4 kJ, effectively delivering over 16 kJ to the first NIF targets. On PDS we demonstrated 3ω operation at energy levels up to 10.4 kJ in a flat-in-time 3.5 ns pulse (equivalent to 2 MJ for full NIF, meeting the NIF 1.8 MJ design requirement). Frequency doubling to 2ω was tested by removing the tripling crystal in PDS and reducing the doubler tuning angle tuning offset to $\sim 120 \mu\text{rad}$ for best performance. The doubler crystal edges were also beveled to mitigate transverse Stimulated Brillouin Scattering. Frequency doubling was tested in PDS at energy levels up to 11.4 kJ/beam in a flat-in-time 5 ns pulse, even though the thickness of the available 11 mm doubler used for this campaign was not optimized for high efficiency doubling. Figure 12 shows observed conversion efficiency versus incident 1ω drive for the two configurations described above, along with model calculations. Figure 13 shows near field images for the highest energy 2ω and 3ω shots, both demonstrating adequate beam quality.

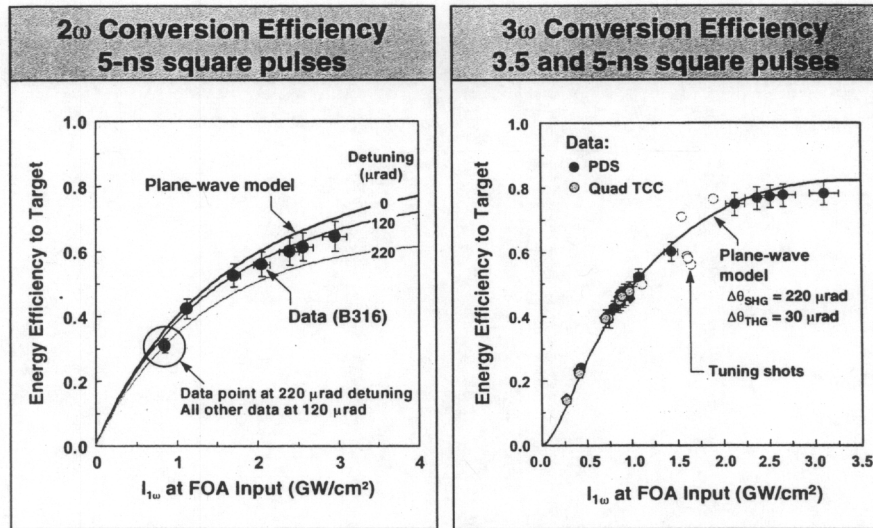


Fig. 12 Observed conversion curves to the green and the blue using square drive pulses with pulse lengths of 5 resp. 3.5 ns. along with model predictions.

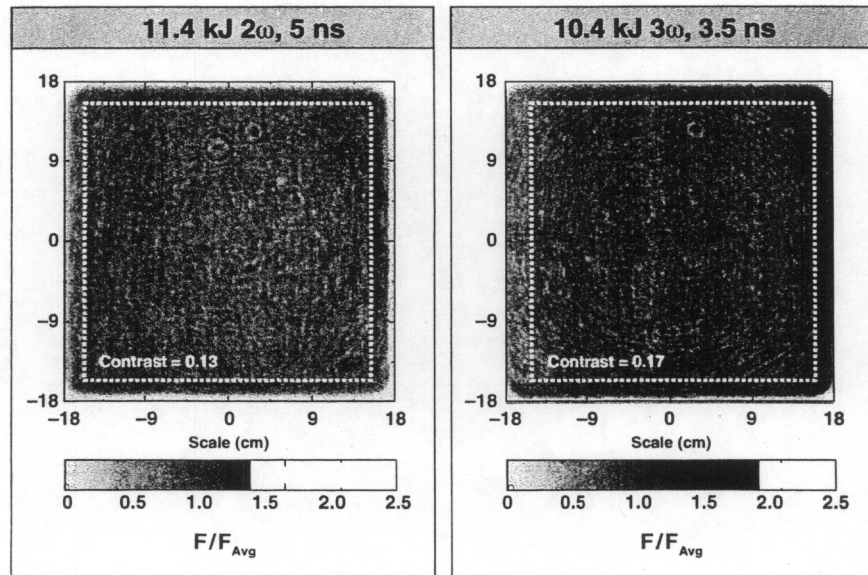


Fig. 13. Near field images of high energy 2ω , and 3ω shots obtained in the NIF Precision Diagnostic System

A critical requirement for NIF is the capability to accurately and reproducibly generate temporally shaped pulses as required by the specific experiment. This is achieved by calculating the MOR pulse shape for each quad using a calibrated model (LPOM) and a high dynamic range arbitrary waveform generator in the MOR to create the calculated input pulse. The most demanding tests so far included long, flat in time pulses, as shown in Fig. 13, and highly shaped ignition pulses, such as the Suter pulse at 2ω shown in Fig. 14. Agreement between requested and observed pulse shape is excellent. Additional pulse shaping requirements such as short pulse generation (200 ps) and fast rise time flat in time pulses have also been demonstrated.

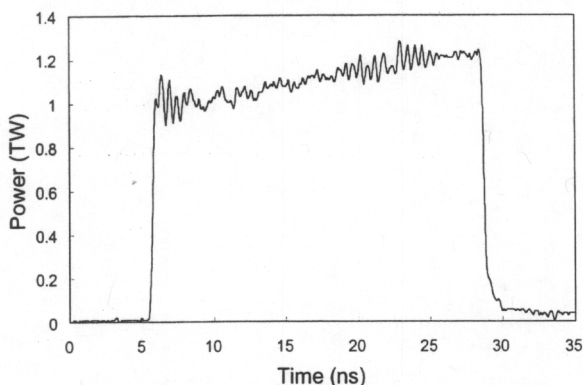


Fig. 14. Output power versus time for a 26 kJ energy long 23 ns pulse.

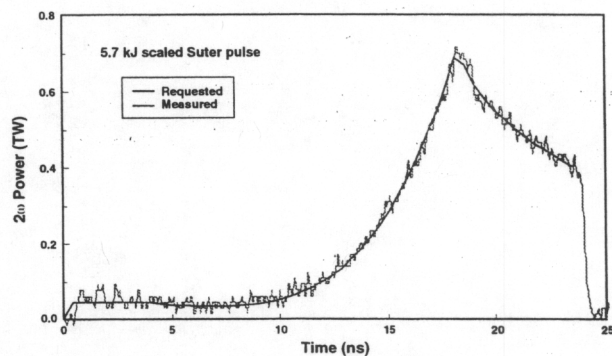


Fig. 15. Comparing observed and requested output Power for a highly shaped Suter pulse at 2ω

The successful generation of high energy long pulses also demonstrated the absence of pinhole closure effects in the main laser transport spatial filters. Time resolved contrast measurements of a streaked section of the near field show a continuous decrease of the contrast over time, rather than an abrupt rise near the end of the pulse. This is not unexpected as the mitigation of pinhole closure by the use of long conical pinholes was developed and proven on the Beamlet prototype facility¹³.

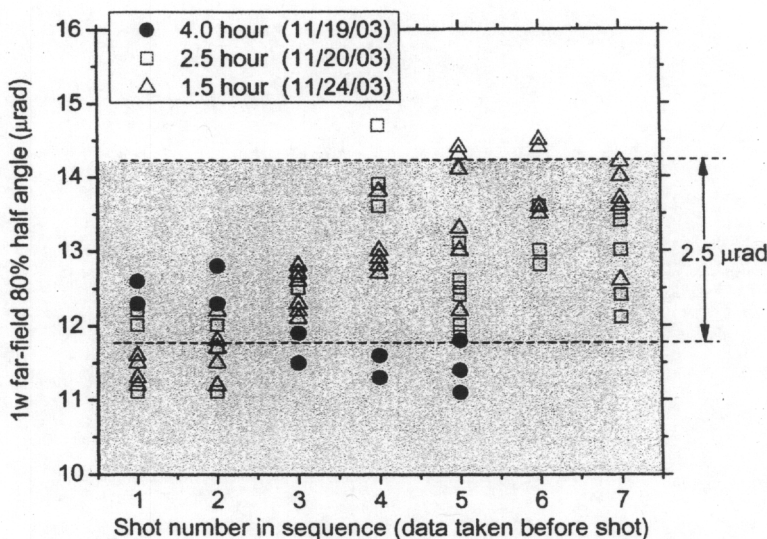


Figure 14. Preshot far-field spot size measured as a function of shot numbers for three different shot rates ranging from 1.5 hour to 4 hours. The indicated $2.5 \mu\text{rad}$ band is the NIF requirement for uncompensated thermal effects.

NEL was also used to test the NIF shot rate capabilities as limited by thermal effects caused by heat build-up in the main amplifiers. Heat deposition causes both slow low frequency wavefront aberrations as a consequence of slab distortion, and fast higher spatial frequency aberrations caused by gas motion (buoyancy) in the beampath. To mitigate this effect, a sophisticated high capacity amplifier cooling system was designed and installed. The amplifier cooling systems consists of a flashlamp cooling system to quickly remove the heat from the hot flashlamps before it radiatively couples to the slabs, and an amplifier purge/slab cooling system. The amplifier cavity purge removes aerosols formed after firing the flashlamp. Fig. 14 shows the results of a recent shot rate campaign. The focal spot size of the pulsed beam was measured right before shot time during a sequence of shots fired at three different rates: 4 hours (2.3 hours of flashlamp cooling), 2.5 hours (50 minutes of flashlamp cooling), and 1.5 hours (30 minutes of flashlamp cooling). The data shows little thermal effects at a 4 hour shot rate, demonstrating the NIF requirements for an 8 hour shot rate with a goal of 4 hours. The effect on spot size for 1.5 and 2.5 hr shot rates are rather small and close to the 2.5 μ m allowance for uncorrectable thermal effects. At the highest shot rate, the limiting factor may become heat build-up in the slabs.

CONCLUSION

The Early Light Project demonstrated the successful installation and commissioning of a full quad (4 beam lines) of the 192 beam National Ignition facility laser all the way from the master oscillator to a target located at the center of the target chamber. The commissioning sequence and activities were executed as planned, proving the viability of the major design assumptions: clean beampath assembly and support structure pre-alignment, LRU pre-alignment and off-line testing along with their clean transport and installation. Using the Precision Diagnostic System, individual beam line performance was demonstrated to meet or exceed all major NIF requirements in terms of power, energy and pulse length and setting record Nd:glass energies of 26 kJ at 1 ω (5 MJ NIF equivalent), 11.4 kJ at 2 ω (2.2 MJ NIF equivalent) and 10.4 kJ at 3 ω (2MJ NIF equivalent).

REFERENCES

1. B. Van Wonterghem et al., "Performance of a prototype for a large-aperture multipass Nd:glass laser for inertial confinement fusion", *Applied Optics*, 36(21), 4932 (1997).
2. R. Zacharias et al., "NIF alignment and wavefront control", these proceedings.
3. J. Wisoff et al., "NIF Injection Laser System", these proceedings.
4. S. Skupsky et al., "Improved laser-beam uniformity using the angular dispersion of frequency-modulated light", *J. Appl. Phys.*, 66, 3456 (1989).
5. P. Arnold et al., "NIF Plasma Electrode Plasma Cell", these proceedings.
6. M.A. Rhodes, et al., "Plasma Electrode Pockels Cell for the National Ignition Facility", UCRL-JC-129710, *Proc. of the 3rd Intl. Conf. on Solid State Lasers for Inertial Confinement Fusion*, Monterey, CA, June 1998.
7. P.J. Wegner, "Final Optics: frequency conversion and beam conditioning", these proceedings.
8. J.A. Caird et al., "Beamlet Focal Plane Diagnostic", *Proceedings of the 2nd Annual International Conference on Solid State Laser for Application to Inertial Confinement Fusion*, SPIE Vol. 3047, 237 (1996).
9. W. Williams et al., "Optical Propagation Modeling", these proceedings.
10. M. Shaw et al., "Laser Performance Optics Model (LPOM)", these proceedings.
11. L. Suter et al., "Exploring the limits of the National Ignition Facility's capsule coupling", *Physics of Plasmas*, 7, 2092 (2000).
12. J.E. Murray et al., "Spatial Filter Pinhole Development for the National Ignition Facility", *Applied Optics*, 39(6), 1405 (2000).

* Work performed in collaboration with the United Kingdom Ministry of Defence as part the Shot Rate Enhancement Program (SREP) and under the auspices of the U.S. DOE by UC, LLNL under contract No. W-7405-Eng-48.